

Micro Image Classification of 19 High-value Hardwood Species Based on Texture Feature Fusion

Xiaoxia Yang,^a Hailan Jiang,^a Lixin Ma,^a Wenhui Yang,^{a,*} Xiaohan Zhao,^a Cuiping Hu,^b and Zhedong Ge^c

For classification of wood species with similar microstructure, 19 high-value hardwood species of Papilionaceae, Ebenaceae, and Caesalpiniaceae were used as experimental objects. Images of transverse sections, radial sections, and tangential sections were collected by Micro CT. Local binary patterns (LBP) are often used for feature extraction. LBP deformed forms such as uniform LBP, rotation-invariant LBP, and rotation-invariant uniform LBP were fused with Gray-Level Co-Occurrence Matrix (GLCM) to form three fusion features. The fusion features were combined with support vector machine (SVM) or BP neural network to realize wood classification. The texture feature fusion method was found to be better than the single feature classification. Among them, the effect of uniform LBP and GLCM fusion was the best, and the classification accuracy combined with SVM was the highest. The evaluation of the classification of 19 kinds of hardwood mainly depended on transverse sections, and its accuracy was higher than that of the radial and tangential sections. Therefore, the classification results of transverse sections should be taken as the main evaluation basis for the classification of the 19 high-value hardwood species.

DOI: 10.15376/biores.18.2.3373-3386

Keywords: High-value hardwood; Feature fusion; Texture feature; Image classification

Contact information: a: School of New Generation Information Technology Industry, Shandong Polytechnic, Jinan, Shandong 250101 China; b: Linshu County Garden Sanitation Guarantee Service Center, Linyi, Shandong 276700 China; c: School of Information and Electrical Engineering, Shandong Jianzhu University, Jinan, Shandong 250101, China; *Corresponding author: Yang_mess@163.com

INTRODUCTION

Wood has renewable and environmentally friendly advantages. It can be used as the raw material for flooring, furniture, buildings, and interior decoration. Its use is related to the species and features. Many high-value species with better quality are imported from abroad, so it is of great significance for wood to be classified correctly. Traditionally, experts slice the wood and use optical light microscopy to observe its transverse sections, radial sections, and tangential sections (Barmpoutis *et al.* 2018; Jahanbanifard *et al.* 2020). However, this method is cumbersome, time-consuming, and requires highly trained professionals. In this paper, micro computed tomography (micro CT) was used to collect high-resolution microscopic images. This is a more advanced method that allows faster collection of data. Large numbers of images on the three sectional planes are collected in a very short time. These abundant images are the premise of wood classification and identification by computer vision and machine learning. At present, the majority of species identification is completed by computer vision with digital images (Hu *et al.* 2019; Cao *et al.* 2021; Fabijańska *et al.* 2021), which is more efficient and accurate than the traditional

method (Kamal *et al.* 2017).

Machine learning and pattern recognition have been applied to macroscopic and microscopic images recognition of wood, and the method of texture feature extraction is widely used in wood classification (Zhao *et al.* 2014). Local phase quantization and linear discriminant method were used to classify 77 commercial timber species, and the average success rate was approximately 88% (Rosa *et al.* 2017). Local binary patterns (LBP) combined with support vector machine (SVM) were used to classify 2240 microscopic images of 112 wood species, and the accuracy reached 98.6% (Martins *et al.* 2013). Rotation-invariant LBP and SVM were used to classify 46 Brazilian species, and the accuracy reached 97.67%. By using the fusion of classifiers, the accuracy rate was improved by 0.33% (Souza *et al.* 2020). Six texture feature extraction techniques and three classifiers were used to classify hardwood species images. The results showed that the reduced dimension texture feature uniform completed local binary pattern (DWTCCLBPu2) combined with LDA classifier had the best classification accuracy (Yadava *et al.* 2015). A multi-resolution texture classification method based on anisotropic diffusion and local directional binary pattern (LDBP) was used to evaluate and compare four texture data sets, and the results showed its effectiveness (Hiremath *et al.* 2017).

In addition to LBP, by using Gray Level Co-Occurrence Method (GLCM) and Euclidean distance method to identify the swietenia mahagoni wood defects, the optimal average accuracy reached 88.90% (Riana *et al.* 2021). The Improved-Basic Gray Level Aura Matrix (I-BGLAM) feature extraction method was proposed, and the back-propagation neural network classifier was used to realize the automatic classification of 52 kinds of wood (Zamri *et al.* 2016). The Lucy Richardson algorithm was used to enhance blurred images, the statistical feature extraction technology and SVM were used to identify 20 tropical wood species, and the classification accuracy reached 89.3% (Rajagopal *et al.* 2019). A new Gabor method for wood recognition was proposed, and the method was evaluated on the wood database of Zhejiang Agriculture and Forestry University (ZAFU), which show that the method had achieved progress relative to the state of the art (Wang *et al.* 2013). LBP and GLCM were used to extract features through X-ray tomography, and K-Nearest Neighbor (KNN) classifier was employed in order to classify six kinds of diffuse porous wood (Kobayashi *et al.* 2019). A method of combining Tamura and GLCM texture features was proposed, and BP neural network was used to classify the wood surface defects, thus improving the accuracy and robustness of recognition (Xie and Wang 2015).

The above-cited scholars took transverse sections as the object, but the radial and tangential sections also provide a lot of information. Barmoutis *et al.* (2018) proposed a new approach for automating wood species recognition through multidimensional texture analysis. The accuracy performance of transverse-section classification was 91.47% and 84.2% for radial and tangential sections. Up to the present, there have been few studies on classification and recognition of high-value hardwood species from the transverse, radial, and tangential sections. In this paper, three-section images of 2 μm resolution were obtained by Micro CT, and 19 hardwood species with similar structure were classified and recognized. In this work, LBP deformation forms uniform LBP, rotation-invariant LBP, and rotation-invariant uniform LBP were fused with GLCM features to form three fusion features. Compared with a single texture feature, three fusion features combined with SVM and BP neural network showed the highest accuracy and the best recognition effect. Among them, the uniform LBP and GLCM fusion method was the optimum. Combined with SVM and BP neural network, it achieved the best classification effect on the transverse, radial and tangential sections.

EXPERIMENTAL

Materials

The experimental materials were taken from the Specimens Museum of the Shandong Jianzhu University (Jinan China). A total of 19 kinds of hardwood with similar micro-structure were selected, and the samples were cut to 2.5 mm × 2.5 mm × 25 mm for scanning. The Bruker Kscan1272 was used for scanning, and the voltage and current values of the radiation source were set to 50 kV and 200 μA. A total of 3000 images were obtained from each sample, 1000 for transverse sections, 1000 for radial sections, and 1000 for tangential sections. The size was 2042 × 1640 pixels, and the resolution was 2 μm. Table 1 shows the 19 high-value hardwood species.

Table 1. Information Related to the High-value Hardwood Species under Study

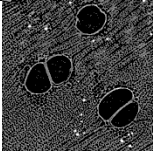
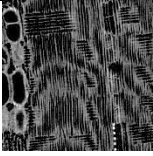
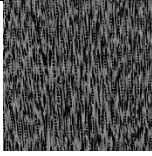
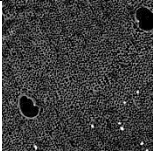
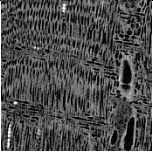
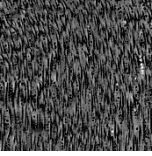
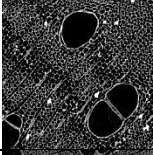
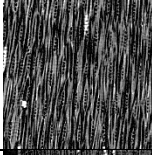
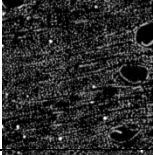
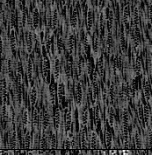
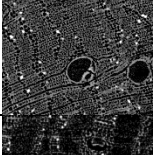
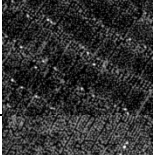
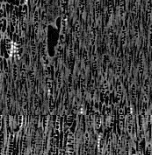
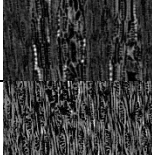
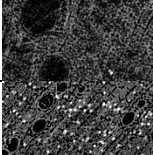
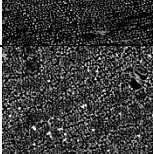
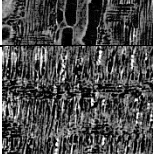
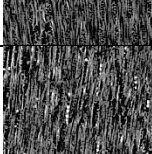
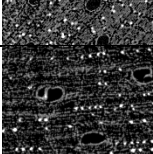
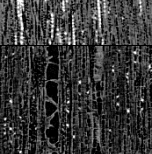
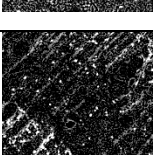
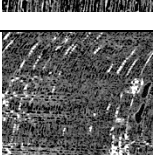
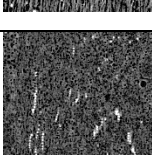
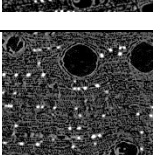
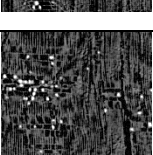
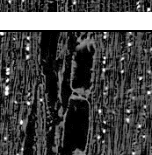
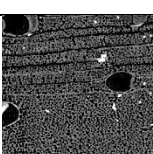
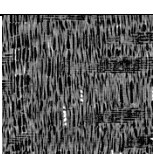
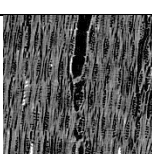
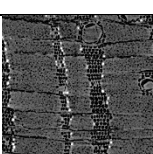
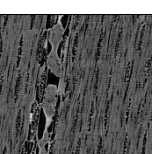
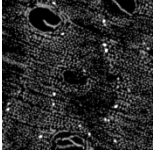
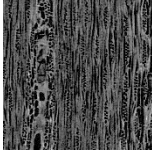
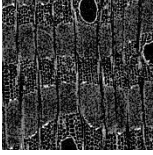
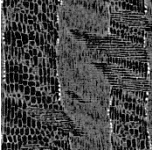
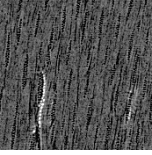
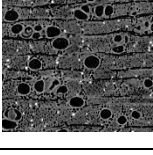
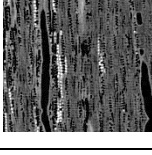
No.	Botanical name	Category	Producer	Botanical family
1	<i>Pterocarpus erinaceus</i>	Diffuse-porous	Africa	Papilionaceae
2	<i>Pterocarpus indicus</i>	Diffuse-porous	Indonesia	Papilionaceae
3	<i>Pterocarpus macrocarpus</i>	Diffuse-porous	Myanmar	Papilionaceae
4	<i>Dalbergia cultrata</i>	Diffuse-porous	Myanmar	Papilionaceae
5	<i>Dalbergia latifolia</i>	Diffuse-porous	Indonesia	Papilionaceae
6	<i>Dalbergia louvelii</i> R. Vig.	Diffuse-porous	Madagascar	Papilionaceae
7	<i>Dalbergia melanoxylon</i>	Diffuse-porous	Tanzania	Papilionaceae
8	<i>Dalbergia stevensonii</i> Standl.	Semi-ring porous wood	Mexico	Papilionaceae
9	<i>Dalbergia bariensis</i> Pierre	Diffuse-porous	Laos	Papilionaceae
10	<i>Dalbergia cearensis</i> Ducke	Diffuse-porous	Brazil	Papilionaceae
11	<i>Dalbergia cochinchinensis</i> Pierre	Diffuse-porous	Laos	Papilionaceae
12	<i>Dalbergia frutescens</i> Var.	Diffuse-porous/ Semi-ring porous wood	Myanmar	Papilionaceae
13	<i>Dalbergia oliveri</i> Prain	Diffuse-porous/ Semi-ring porous wood	Myanmar	Papilionaceae
14	<i>Dalbergia retusa</i> Hemsl.	Diffuse-porous	Nicaragua	Papilionaceae
15	<i>Diospyros ebenum</i> J.	Diffuse-porous	Philippines	Ebenaceae
16	<i>Diospyros celebica</i> Bakh	Diffuse-porous	Sulawesi	Ebenaceae
17	<i>Diospyros philippinensis</i> A.DC.	Diffuse-porous	Philippines	Ebenaceae
18	<i>Millettia leucantha</i>	Diffuse-porous	Myanmar	Papilionaceae
19	<i>Senna siamea</i> (Lam.)	Diffuse-porous	Myanmar	Caesalpiniaceae

Dataset Construction

A total of 300 images were randomly selected from the three sections of the 19 wood species, 100 images for each section. The selected images were cut randomly into sub-images with size of 500 × 500 pixels, which were used to construct the three-section data sets. In sum, there were 5700 microscopic sub-images obtained, 1900 sub-images for each section.

Table 2 shows the microscopic images of transverse, radial, and tangential sections. A variety of structures are seen in the microscopic images, such as vessel pores, axial parenchyma, wood rays, etc.

Table 2. The Three-Section Images of 19 High-Value Hardwood Species

No	Transverse Sections	Radial Sections	Tangential Sections	No	Transverse Sections	Radial Sections	Tangential Sections
1				11			
2				12			
3				13			
4				14			
5				15			
6				16			
7				17			
8				18			
9				19			
10							

Feature Fusion

The surface of wood is distributed with different structures, which constitute the texture of wood, and the texture distribution of different sections varies greatly. In this work, a method is proposed, namely a texture feature fusion for uniform *LBP*, rotation-invariant *LBP*, and a rotation-invariant uniform *LBP* that is fused with *GLCM*. The fusion method is as follows:

To reduce the *LBP* dimension and shorten the calculation, 90% texture modes and information of the microscopic images were grouped to construct Uniform *LBP* (Ojala *et al.* 2002, 2013). The *U* value was limited to being no greater than 2, and calculation was carried out using Eq. 1:

$$LBP_{P,R}^{U,2} = |s(g_{p-1} - g_c) - s(g_0 - g_c)| + \sum_{i=1}^{P-1} |s(g_i - g_c) - s(g_{i-1} - g_c)| \tag{1}$$

To maintain the rotation of *LBP*, the circular neighborhood was rotated one circle clockwise to generate different binary codes. Take the minimum value in the codes as the Uniform *LBP* to describe the invariant rotation feature. The $LBP_{P,R}^{U,2}$ formula is as follows.

$$LBP_{P,R}^{ri} = \min\{ROR(LBP_{P,R}^{ri}, i), i = 0, 1, \dots, P - 1\} \tag{2}$$

Combining with the above process, the Uniform *LBP* with invariant rotation feature is constructed, and the formula is as follows.

$$LBP_{P,R}^{riu2} = \begin{cases} \sum_{i=0}^{P-1} s(g_i - g_c), U(LBP_{P,R}) \leq 2 \\ P + 1 \end{cases} \tag{3}$$

The radius *P* is equal to 8, and the feature dimensions of $LBP_{P,R}^{U,2}$, $LBP_{P,R}^{ri}$, $LBP_{P,R}^{riu2}$ are 59, 36, and 10, respectively.

Based on the *GLCM*, five features were obtained, including energy, contrast (*CON*), correlation (*COR*), entropy (*ENT*), and inverse difference moment (*IDM*). According to these features, feature data sets of 64, 41, and 15 dimensions were constructed for each image. Comparing with traditional *LBP*, this method is lightweight, and it reflects the *IDM* of texture images in gray distribution, the differences among textures, the similarity of rows' and columns' gray values, the complexity, and roughness of textures (Haralick 1979).

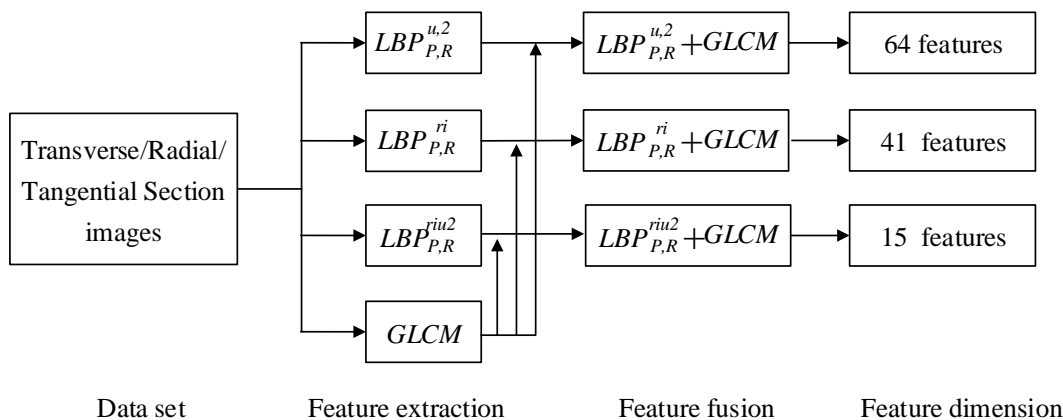


Fig. 1. Feature fusion

In this paper, uniform *LBP*, rotation-invariant *LBP*, and rotation-invariant uniform *LBP* were fused with *GLCM* texture features, and are expressed as $LBP_{P,R}^{ri} + GLCM$,

$LBP_{P,R}^{riu^2}+GLCM$, $LBP_{P,R}^{u^2}+GLCM$, as shown in Fig. 1. The method of texture feature fusion can integrate all kinds of information in the image and improve the classification accuracy (Yusof *et al.* 2010; Yan *et al.* 2021).

Classification

According to the three fused features, namely $LBP_{P,R}^{ri}+GLCM$, $LBP_{P,R}^{riu^2}+GLCM$, and $LBP_{P,R}^{u^2}+GLCM$, the BP neural network and SVM were used for classification. The data of training set and testing set were 70% and 30%, respectively.

The BP neural network was set up as a three-layer network structure, including an input layer, a hidden layer, and an output layer. The number of features of each image in the input layer was 59, 36, 10, 64, 41, 15, the number of neurons in the hidden layer was 5, 10, 15, 20, 25, 30, 35, 40, and the classification accuracy of 19 species was in the output layer. The input layer to hidden layer activation function was tanh, and the hidden layer to output layer activation function was Purelin. The training times were 1000 and the learning rate was 0.01, the error rate was 0.00001, the momentum parameter was 0.01, and the minimum performance gradient was $1e-6$. The structure of BP neural network is shown in Fig. 2.

The SVM was based on LIBSVM software package, and the Radial Basis Function (RBF) was applied. The value range of penalty factor C and kernel parameter g was 2-10-210 (Chih and Lin 2011). The number of features of each image imported was 59, 36, 10, 64, 41, and 15. These numbers were randomly arranged, and 5-fold cross validation was used to determine the optimal values of C and g. Then the classification accuracy for the 19 species was output.

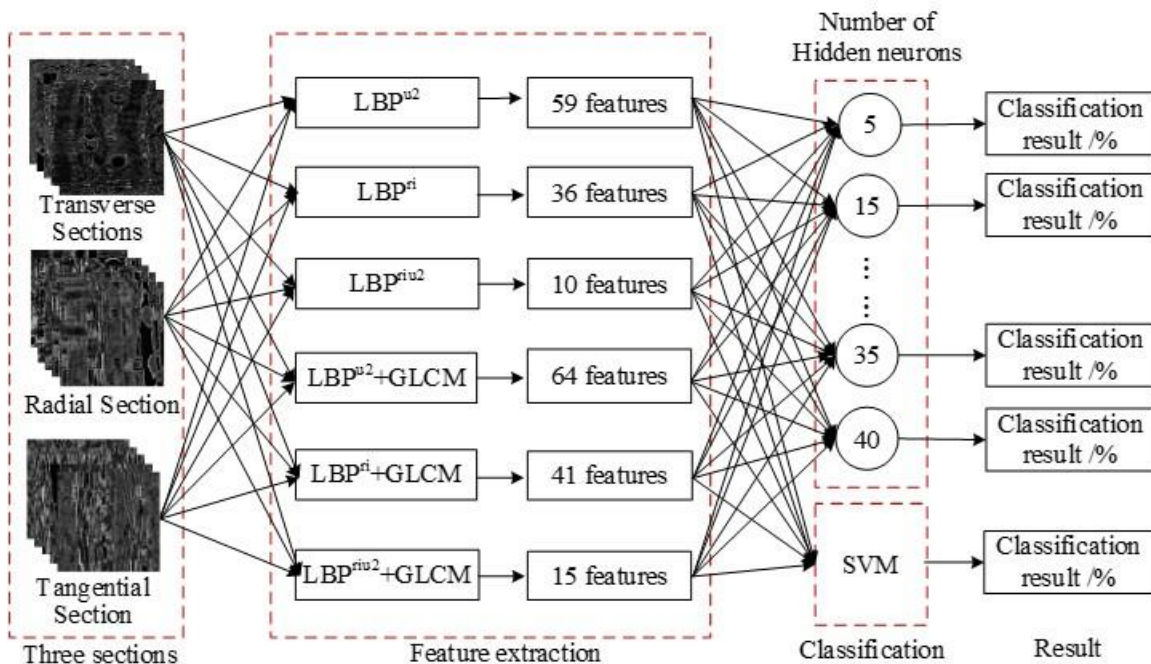


Fig. 2. Classification structure of BP neural network and SVM

RESULTS AND DISCUSSION

BP Neural Network

During the classification by BP neural network, the number of neurons in the hidden layer affects the classification accuracy. Table 3 shows the maximum classification accuracy and time point corresponding to the number of optimal hidden-layer neurons with different features. The increase of feature dimension leads to more time required for classification. In the classification of single feature, the accuracy of $LBP_{P,R}^{ri}$ in transverse, radial, and tangential sections was 94.73%, 86.77%, and 86.39%. The accuracy of $LBP_{P,R}^{riu,2}$ in three-section was 93.50%, 86.28%, and 85.96%. The accuracy of $LBP_{P,R}^{iu,2}$ in three-section was 95.78%, 88.19%, and 88.05%. In the classification of single feature, the training time used by $LBP_{P,R}^{riu,2}$ was shorter, but the accuracy was low. $LBP_{P,R}^{iu,2}$ exhibited the highest classification accuracy in transverse, radial, and tangential sections, and the classification effect was relatively good.

After feature fusion of the classification of transverse, radial, and tangential sections, the accuracy of $LBP_{P,R}^{ri}+GLCM$ increased by 0.7%, 3.75%, and 1.68% in comparison to $LBP_{P,R}^{ri}$, the accuracy of $LBP_{P,R}^{riu,2}+GLCM$ increased by 1.23%, 3.19%, and 0.88% in comparison to $LBP_{P,R}^{riu,2}$, and the accuracy of $LBP_{P,R}^{iu,2}+GLCM$ increased by 1.58%, 3.21%, and 2.03% in comparison to $LBP_{P,R}^{iu,2}$, respectively. These findings indicate that the classification result of $LBP_{P,R}^{iu,2}+GLCM$ was the best, and the classification accuracy for the three-section set of images was able to reach over 90%.

Table 3. Classification Results of BP Neural Network

Section	Feature	Hidden Neuron	Accuracy (%)	Time (s)	Feature Fusion	Hidden Neuron	Accuracy (%)	Time (s)
Transverse	$LBP_{P,R}^{ri}$	35	94.73	80	$LBP_{P,R}^{ri}+GLCM$	35	95.43	135
	$LBP_{P,R}^{riu,2}$	20	93.50	15	$LBP_{P,R}^{riu,2}+GLCM$	40	94.73	203
	$LBP_{P,R}^{iu,2}$	25	95.78	152	$LBP_{P,R}^{iu,2}+GLCM$	20	97.36	83
Radial	$LBP_{P,R}^{ri}$	40	86.77	78	$LBP_{P,R}^{ri}+GLCM$	30	90.52	127
	$LBP_{P,R}^{riu,2}$	35	86.28	56	$LBP_{P,R}^{riu,2}+GLCM$	25	89.47	35
	$LBP_{P,R}^{iu,2}$	30	88.19	89	$LBP_{P,R}^{iu,2}+GLCM$	30	91.40	224
Tangential	$LBP_{P,R}^{ri}$	30	86.39	75	$LBP_{P,R}^{ri}+GLCM$	40	88.07	251
	$LBP_{P,R}^{riu,2}$	35	85.96	54	$LBP_{P,R}^{riu,2}+GLCM$	40	86.84	135
	$LBP_{P,R}^{iu,2}$	40	88.05	93	$LBP_{P,R}^{iu,2}+GLCM$	30	90.08	213

As shown in Fig. 3, the accuracy of transverse sections classification using the above 6 feature classification methods were much higher than that of radial and tangential sections. Therefore, the classification results of transverse sections should be considered in the process of tree species classification. The results of wood species classification on the three sections showed that the accuracy of the $LBP_{P,R}^{riu,2}$ method was the lowest, and the accuracy of the $LBP_{P,R}^{iu,2}+GLCM$ combination after feature fusion was the highest. After feature

fusion, the classification accuracy of $LBP_{P,R}^{ri}+GLCM$, $LBP_{P,R}^{riu,2}+GLCM$, $LBP_{P,R}^{iu,2}+GLCM$ was generally higher than that of single feature such as $LBP_{P,R}^{ri}$, $LBP_{P,R}^{riu,2}$, $LBP_{P,R}^{iu,2}$. As the increase of feature dimension can improve the classification accuracy, the results considering both classification accuracy and time point after extension of time showed that, for the 19 kinds of high-value hardwood species and 6 feature classification methods, $LBP_{P,R}^{iu,2}+GLCM$ performed the best in accuracy and time.

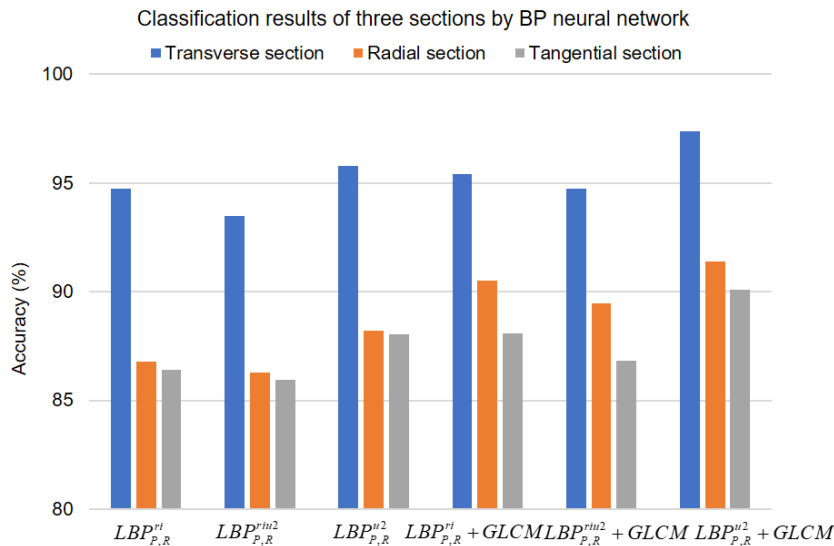


Fig. 3. Classification results of the three sections (transverse, radial, and tangential) by BP neural network

Support Vector Machine (SVM)

The classification results of 19 high-value hardwood by SVM classifier are shown in Table 4. In the classification of single feature, the accuracy of $LBP_{P,R}^{ri}$ in transverse, radial, and tangential sections was 94.92%, 90.52%, and 90.05%, respectively. The accuracy of $LBP_{P,R}^{riu,2}$ in the three sections was 93.68%, 90.70%, and 89.82%, respectively. The accuracy of $LBP_{P,R}^{iu,2}$ in the three sections was 95.27%, 91.40%, and 91.40%, respectively. In the classification of single feature, the training time used by $LBP_{P,R}^{riu,2}$ was shorter, but the accuracy rate was low. $LBP_{P,R}^{iu,2}$ achieved the highest classification accuracy in transverse, radial, and tangential sections, and the classification effect was relatively good.

After feature fusion of the three sections, the classification accuracies of $LBP_{P,R}^{ri}+GLCM$ were increased by 1.04%, 0.70%, and 1.17% compared to $LBP_{P,R}^{ri}$, and the accuracies of $LBP_{P,R}^{riu,2}+GLCM$ were increased by 0.88%, 1.05%, and 0.7% compared to $LBP_{P,R}^{riu,2}$, and the accuracies of $LBP_{P,R}^{iu,2}+GLCM$ were increased by 2.27%, 0.88%, and 0.17% compared to $LBP_{P,R}^{iu,2}$. This shows that the accuracy of the three sections by $LBP_{P,R}^{iu,2}+GLCM$ were all about to reach 91%. The result shows that the classification result of $LBP_{P,R}^{iu,2}+GLCM$ was the best and can be used as the main reference for wood classification.

Table 4. Classification Results by SVM

Section	Feature	Accuracy (%)	Time (s)	Feature Fusion	Accuracy (%)	Time (s)
Transverse	$LBP_{P,R}^{ri}$	94.92	3906	$LBP_{P,R}^{ri}+GLCM$	95.96	4097
	$LBP_{P,R}^{riu,2}$	93.68	1674	$LBP_{P,R}^{riu,2}+GLCM$	94.56	2044
	$LBP_{P,R}^{u,2}$	95.27	4586	$LBP_{P,R}^{u,2}+GLCM$	97.54	4834
Radial	$LBP_{P,R}^{ri}$	90.52	3958	$LBP_{P,R}^{ri}+GLCM$	91.22	4226
	$LBP_{P,R}^{riu,2}$	90.70	1582	$LBP_{P,R}^{riu,2}+GLCM$	91.75	2264
	$LBP_{P,R}^{u,2}$	91.40	4597	$LBP_{P,R}^{u,2}+GLCM$	92.28	5339
Tangential	$LBP_{P,R}^{ri}$	90.05	3851	$LBP_{P,R}^{ri}+GLCM$	91.22	3947
	$LBP_{P,R}^{riu,2}$	89.82	1698	$LBP_{P,R}^{riu,2}+GLCM$	90.52	2114
	$LBP_{P,R}^{u,2}$	91.40	4912	$LBP_{P,R}^{u,2}+GLCM$	91.57	4990

Figure 4 shows that the classification accuracy of transverse sections was higher than that of radial and tangential sections by using the above 6 feature classification methods. Pan *et al.* (2021) concluded that *GLCM* incorporated with near-infrared (NIR) spectral features can rapidly identify wood, and that transverse sections contain more distinguishable wood features than the tangential and radial sections.

The results of wood species classification on the three sections showed that the accuracy of the $LBP_{P,R}^{riu,2}$ method was the lowest, and the accuracy of $LBP_{P,R}^{u,2}+GLCM$ method after feature fusion was the highest. The classification accuracy after feature fusion was generally higher than that of single feature. The results considering both classification accuracy and time point showed that $LBP_{P,R}^{u,2}+GLCM$ performed the best for the 6 features of 19 kinds of high-value hardwood.

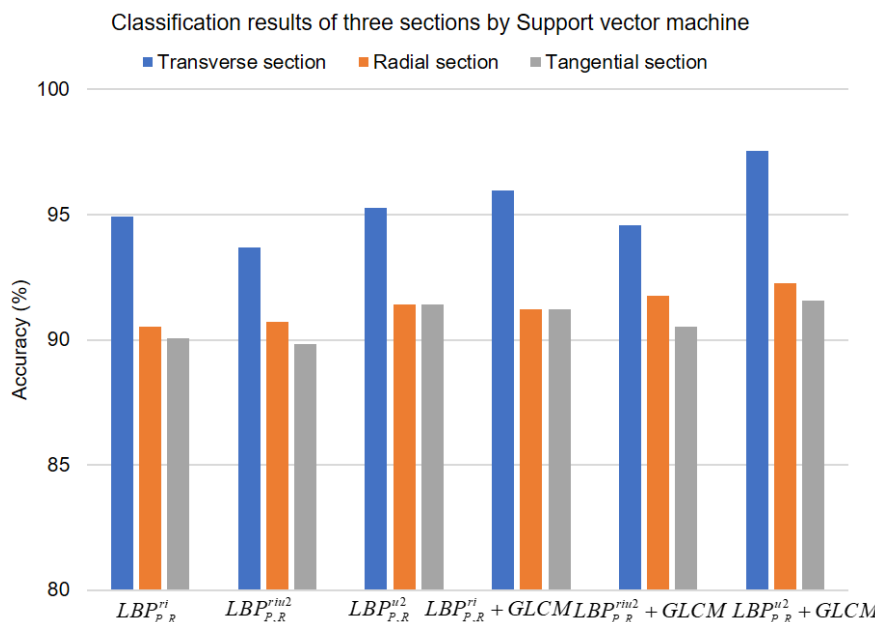


Fig. 4. Classification results of three sections (transverse, radial, and tangential) by SVM

Based on the work carried out, it can be concluded that the classification accuracy after feature fusion was the highest, which is consistent with the other researchers. For example, Nasir *et al.* (2019) classified the thermally modified wood samples, indicating that the fusion of all signal domain features showed the best classification performance. Wang and Zhao (2021) used spectral features and texture features to classify 50 kinds of wood transverse sections. Thus, the feature fusion method is better than a single texture feature or spectral feature, and the accuracy reached 99.16%.

Confusion Matrix and Evaluation Metrics

Compared with BP neural network, the proposed feature fusion method combined with SVM achieved higher classification accuracy. Among the feature fusion methods, $LBP_{P,R}^{U,2} + GLCM$ had the best effect. The best accuracy performances of transverse sections, radial, and tangential sections were 97.54%, 92.28%, and 91.57%, respectively. The confusion matrix of three sections were drawn, as shown in Fig. 5.

As shown in Fig. 5(a), most of the transverse sections classifications of 19 high-value hardwood species were correct, and the accuracy rate was more than 94%. Only the thirteenth species (*Dalbergia oliveri* Prain) had a low accuracy rate of 90%. Three species in the thirteenth species (*D. oliveri* Prain) were classified mistakenly to the third species (*Pterocarpus macrocarpus*). The axial parenchyma of both *D. oliveri* Prain and *P. macrocarpus* were of zonal distribution, and the microstructures were very similar.

As shown in Fig. 5(b), most of the radial-section classifications of 19 high-value hardwood species were correct, and the accuracy rate was more than 85%. Only the 4th (*Dalbergia cultrate*) and 14th species (*Dalbergia retusa* Hemsl) got lower accuracy rates of 84% and 81%. Some of the species in the fourth were mistakenly classified into the 9th (*Dalbergia bariensis* Pierre), the 11th (*Dalbergia cochinchinensis* Pierre), the 14th (*Dalbergia retusa* Hemsl), and the 19th (*Senna siamea* (Lam.)). Some of the species in the 14th were mistakenly classified into the 4th (*Dalbergia cultrate*), the 7th (*Dalbergia melanoxyton*), the 16th (*Diospyros celebica* Bakh), and the 19th (*Senna siamea* (Lam.)) The reason is that *Dalbergia cultrate*, *Dalbergia melanoxyton*, *Dalbergia bariensis* Pierre, *Dalbergia cochinchinensis* Pierre and *Dalbergia retusa* Hemsl are all belong to *Dalbergia* and have much similarity in microstructure.

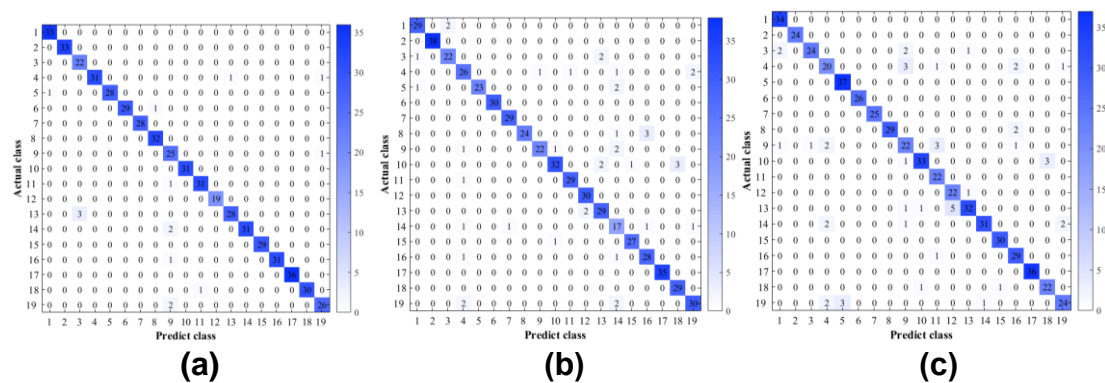


Fig. 5. The confusion matrix for sections: (a) Transverse sections in the first panel; (b) Radial sections in the second panel; (c) Tangential sections in the third panel

As shown in Fig. 5(c), most of the tangential-section classifications of 19 high-value hardwood species were correct, and the accuracy was more than 80%. Only the 4th

(*Dalbergia cultrate*) and 9th species (*Dalbergia bariensis* Pierre) got lower accuracy rates of 74% and 73%. Some species in the 4th (*Dalbergia cultrata*) were mistakenly classified into the 9th (*Dalbergia bariensis* Pierre), the 11th (*Dalbergia cochinchinensis* Pierre), the 16th (*Diospyros celebica* Bakh), and the 19th (*Senna siamea* (Lam.)). Some of the species in the 9th (*Dalbergia cultrata*) were mistakenly classified into the 1st (*Pterocarpus erinaceus*), the 3rd (*Pterocarpus macrocarpus*), the 4th (*Dalbergia cultrata*), the 11th (*Dalbergia cochinchinensis* Pierre), and the 16th (*Diospyros celebica* Bakh). The reason is that the ray cell and vessel distributions of these species have much similarity.

The PREC (Precision), REC (Recall), and SPEC (Specificity) parameters were used to evaluate the classification performance.

$$\text{PREC} = \text{TP} / (\text{TP} + \text{FP});$$

$$\text{REC} = \text{TP} / (\text{TP} + \text{FN});$$

$$\text{SPEC} = \text{TN} / (\text{TN} + \text{FP}).$$

TP indicates that the real sample and the predicted sample are both positive. TN indicates that the real sample and the predicted sample are both negative. FN indicates that the real sample is positive and the predicted sample is negative. FP indicates that the real sample is negative and the predicted sample is positive.

Table 5 shows the evaluation values of PREC, REC, and SPEC for each of the 19 species. The average accuracies of transverse sections were 97.42%, 97.32%, and 99.85%, the average accuracies of radial sections were 93.09%, 92.74%, and 99.62%, and the average accuracies of tangential sections were 91.84%, 91.47%, and 99.53%. These results indicate that the PREC, REC, and SPEC values of transverse sections were the highest and the classification accuracy was the best, while the tangential sections got the lowest evaluation values and the worst classification results.

Table 5. The Classification Performance of Three Sections

No.	Transverse sections			Radial sections			Tangential sections		
	PREC (%)	REC (%)	SPEC (%)	PREC (%)	REC (%)	SPEC (%)	PREC (%)	REC (%)	SPEC (%)
1	100.00	97.22	100.00	100.00	93.55	99.63	100.00	91.89	100.00
2	100.00	100.00	100.00	100.00	100.00	100.00	100.00	100.00	100.00
3	100.00	88.00	100.00	88.00	91.67	99.45	82.76	96.00	99.08
4	93.94	100.00	99.62	83.87	81.25	99.07	74.07	76.92	98.71
5	96.55	100.00	99.82	88.46	100.00	99.45	100.00	92.50	100.00
6	96.67	100.00	99.82	100.00	100.00	100.00	100.00	100.00	100.00
7	100.00	100.00	100.00	100.00	96.67	100.00	100.00	100.00	100.00
8	100.00	96.97	100.00	85.71	100.00	99.27	93.55	100.00	99.63
9	96.15	80.65	99.82	84.62	95.65	99.27	73.33	73.33	98.52
10	100.00	100.00	100.00	88.89	94.12	98.88	89.19	94.29	99.25
11	96.88	96.88	99.82	96.67	96.67	99.82	100.00	81.48	100.00
12	100.00	100.00	100.00	100.00	93.75	100.00	95.65	81.48	99.82
13	90.32	96.55	99.45	93.55	87.88	100.00	82.05	94.12	98.69
14	93.94	100.00	99.63	80.95	65.38	99.26	86.11	96.88	99.07
15	100.00	100.00	100.00	96.43	96.43	99.82	100.00	96.77	100.00
16	96.88	100.00	99.82	93.33	87.50	99.63	96.67	85.29	99.81
17	100.00	100.00	100.00	100.00	100.00	100.00	100.00	100.00	100.00
18	96.77	100.00	99.82	100.00	90.63	100.00	91.67	88.00	99.63
19	92.86	92.86	99.63	88.24	90.91	99.26	80.00	88.89	98.90
Avg.	97.42	97.32	99.85	93.09	92.74	99.62	91.84	91.47	99.53

CONCLUSIONS

1. Micro computed tomography (micro CT) was used to collect wood three-section microscopic images with 2 μm resolution. The number and the efficiency of image collection were much better than that of the traditional wood slicing method. The strategy provides abundant images for wood species classification.
2. The accuracy of wood classification obtained by feature fusion method was higher than that of single feature. Among these methods, local binary pattern together with Gray-Level Co-occurrence Matrix ($LBP_{P,R}^{u,2}+GLCM$) in combination with support vector machine (SVM) was the best, which was superior to the back propagation (BP) neural network method.
3. Combining with the above features, the classification accuracy of transverse sections was higher than that of radial and tangential sections no matter whether using BP neural network or SVM. The transverse sections of the same species contain inherent texture information and have stable structure and high similarity, while the transverse sections of different species have great difference in texture. Due to the different angles of image collection of radial and tangential sections, the texture information of the same wood species may be different, which means that the texture information is not stable. Therefore, the classification results of transverse sections should be taken as the main evaluation basis for the classification of the 19 high-value hardwood species.

ACKNOWLEDGEMENTS

The authors are grateful for the youth project of the Shandong Natural Science funds, Project No. ZR2020QC174.

REFERENCES CITED

- Barmpoutis, P., Dimitropoulos, K., Barboutis, I., Grammalidis, N., and Lefakis, P. (2018). "Wood species recognition through multidimensional texture analysis," *Computers and Electronics in Agriculture* 144, 241-248. DOI: 10.1016/j.compag.2017.12.011
- Cao, M. T., Nguyen, N. M., Chang, K. T., Tran, X. L., and Hoang, N. D. (2021). "Automatic recognition of concrete spall using image processing and metaheuristic optimized Logit Boost classification tree," *Advances in Engineering Software* 159, article 103031. DOI: 10.1016/j.advengsoft.2021.103031
- Chih, C. C., and Lin, C. J. (2011). "LIBSVM: A library for support vector machines," *ACM Transactions on Intelligent Systems and Technology* 2(3), 27. DOI: 10.1145/1961189.1961199
- Fabijańska, A., Danek, M., and Barniak, J. (2021). "Wood species automatic identification from wood core images with a residual convolutional neural network," *Computers and Electronics in Agriculture* 181, article 105941. DOI: 10.1016/j.compag.2020.105941
- Haralick, R. M. (1979). "Statistical and structural approaches to texture," *Proceedings of the IEEE* 5(67), 786-804. DOI: 10.1109/proc.1979.11328

- Hiremath, P. S., Bhusnurmath, and Rohini, A. (2017). "Multiresolution LDBP descriptors for texture classification using anisotropic diffusion with an application to wood texture analysis," *Pattern Recognition Letters* 89, 8-17. DOI: 10.1016/j.patrec.2017.01.015
- Hu, J., Song, W., Zhang, W., Zhao, Y., and Yilmaz, A. (2019). "Deep learning for use in lumber classification tasks," *Wood Sci. Technol.* 53, 505-517. DOI: 10.1007/s00226-019-01086-z
- Jahanbanifard, M., Beckers, V., Koch, G., Beeckman, H., Gravendeel, B., Verbeek, F., Baas, P., Priester, C., and Lens F. (2020). "Description and evolution of wood anatomical characters in the ebony wood genus *Diospyros* and its close relatives (Ebenaceae): A first step towards combatting illegal logging," *IAWA Journal* 41(04), 1-43. DOI: 10.1163/22941932-bja10040
- Kamal, K., Qayyum, R., Mathavan, S., and Zafar, T. (2017). "Wood defects classification using laws texture energy measures and supervised learning approach," *Advanced Engineering Informatics* 34, 125-135. DOI: 10.1016/j.aei.2017.09.007
- Kobayashi, K., Hwang, S. W., Okochi, T., Lee, W. H., and Sugiyama, J. (2019). "Non-destructive method for wood identification using conventional x-ray computed tomography data," *J. Cult. Herit.* 38, 88-93. DOI: 10.1016/j.culher.2019.02.001
- Martins, J., Oliveira, L., Nisgoski, S., and Sabourin, R. (2013). "A database for automatic classification of forest species," *Machine Vision and Applications* 24(3), 567-578. DOI: 10.1007/s00138-012-0417-5
- Nasir, V., Nourian, S., Avramidis, S., and Cool, J. (2019). "Stress wave evaluation by accelerometer and acoustic emission sensor for thermally modified wood classification using three types of neural networks," *European Journal of Wood and Wood Products* 77(1), 45-55. DOI: 10.1007/s00107-018-1373-1
- Ojala, T., Pietikainen, M., and Maenpaa, T. (2002). "Multiresolution gray-scale and rotation invariant texture classification with local binary patterns," *IEEE Transactions on Pattern Analysis and Machine Intelligence* 24(7), 971-987. DOI: 10.1109/tpami.2002.1017623
- Ojala, T., Matti, P., and Topi, M. (2013). "A generalized local binary pattern operator for multiresolution gray scale and rotation invariant texture classification," *Advances in Pattern Recognition*. DOI: 10.1007/3-540-44732-6-41
- Pan, X., Li, K., Chen, Z. J., and Yang, Z. (2021). "Identifying wood based on near-infrared spectra and four gray-level co-occurrence matrix texture features," *Forests*. 12, 1527.
- Rajagopal, H., Khairuddin, A. S. M., Mokhtar, N., Ahmad, A., and Yusof, R. (2019). "Application of image quality assessment module to motion-blurred wood images for wood species identification system," *Wood Science and Technology* 53(4), 967-981. DOI: 10.1007/s00226-019-01110-2
- Riana, D., Rahayu, S., Hasan, M., Anton. (2021) "Comparison of segmentation and identification of swietenia mahagoni wood defects with augmentation images," *Heliyon* 7(6), article eo7417.
- Rosa da Silva, N., De Ridder, M., Baetens J. M., Van den Bulcke, J., Rousseau, M., Martinez Bruno, O., Beeckman, H., Van Acker, J., and De Baets, B. (2017). "Automated classification of wood transverse cross-section micro-imagery from 77 commercial Central-African timber species," *Annals of Forest Science* 74(2), 74. DOI: 10.1007/s13595-017-0619-0
- Souza, D. V., Santos, J. X., Vieira, H. C., Naide, T. L., Nisgoski, S., and Oliveira, L. E.

- S. (2020). "An automatic recognition system of Brazilian flora species based on textural features of macroscopic images of wood," *Wood Science and Technology* 54(4), 1065-1090. DOI: 10.1007/s00226-020-01196-z
- Wang, H. J., Qi, H. N., and Wang, X. F. (2013). "A new Gabor based approach for wood recognition," *Neurocomputing* 116, 192-200. DOI:10.1016/j.neucom.2012.02.045
- Wang, C. K., and Zhao, P. (2021). "Classification of wood species using spectral and texture features of transverse section," *European Journal of Wood and Wood Products* 79(5), 1283-1296. DOI: 10.1007/s00107-021-01728-9
- Xie, Y. H., and Wang, J. C. (2015). "Study on the identification of the wood surface defects based on texture features," *Optik* 19(126), 2231-2235. DOI: 10.1016/j.ijleo.2015.05.101
- Yadava, A. R., Ananda, R. S., Dewala, M. L., and Gupta, S. (2015). "Multiresolution local binary pattern variants based texture feature extraction techniques for efficient classification of microscopic images of hardwood species," *Applied Soft Computing* 32, 101-112. DOI: 10.1016/j.asoc.2015.03.039
- Yan, M. Z., Wang, H. Y., Wu, Y. Y., Cao, X. X., and Xu, H. L. (2021). "Detection of chlorophyll content of *Epipremnum aureum* based on fusion of spectrum and texture features," *Journal of Nanjing Agricultural University* 44(3), 568-575.
- Yusof, R., Rosli, N. R., and Khalid, M. (2010). "Using Gabor filters as image multiplier for tropical wood species recognition system," in: *IEEE 2010 12th International Conference on Computer Modelling and Simulation*, Cambridge, UK.
- Zamri, M. I. P., Cordova, F., Khairuddin, A. S. M., Mokhtar, N., and Yusof, R. (2016). "Tree species classification based on image analysis using improved-basic gray level aura matrix," *Computers and Electronics in Agriculture* 124, 227-233. DOI: 10.1016/j.compag.2016.04.004
- Zhao, P., Dou, G., and Chen, G.-S. (2014). "Wood species identification using feature-level fusion scheme," *Optik* 125(3), 1144-1148. DOI: 10.1016/j.ijleo.2013.07.124

Article submitted: January 15, 2023; Peer review completed: February 11, 2023; Revised version received and accepted: March 16, 2023; Published: March 23, 2023.

DOI: 10.15376/biores.18.2.3373-3386